

LCROSS EARLY-TIME EJECTA DISTRIBUTION: PREDICTIONS FROM EXPERIMENTS B. Hermalyn¹, P.H. Schultz¹, and J.T. Heineck², ¹Brown University, Providence, RI 02912-1846 (Brendan_Hermalyn@brown.edu), ²NASA Ames Research Center, Moffet Field, CA 94035

Introduction: The Lunar CRater Observation and Sensing Satellite (LCROSS) mission will use the second stage of the LRO/LCROSS launch vehicle as a kinetic probe to excavate H-bearing materials (specifically in the form of water-ice) from a permanently shadowed region on one of the poles of the moon. In order for the ejected material to be studied, however, a thorough understanding of the ejecta dynamics is necessary. Prior studies have explored the thermal plume[1] and mass/velocity distribution[2] through computational modeling, and general ejecta dynamics through the use of scaling laws[3, 4]. At very early times, however, when the ejecta is moving the fastest, these models and scaling laws break down. Here we present experimental results from the early-time regime as applied to the LCROSS impact event.

Experimental Studies: The impactor, named the Earth-Departure-Upper-Stage (EDUS), will impact the surface at ~ 2.5 km/s at an angle of $\sim 60^\circ$ from horizontal. The trailing Shepherding Spacecraft (SSc) will record the impact and take measurements of the ejecta. As part of a study to understand the effect of impact parameters on the early-stage ejecta distribution, a series of impact experiments were performed at NASA Ames Vertical Gun Range (AVGR). The series of experiments used 12.7mm aluminum projectiles to impact the target surface (#20-30 sand) at ~ 2 km/s at an angle of 60° from horizontal. The EDUS impactor is a hollow cylinder with a low relative density. To study the effect of underdense projectiles, hollow 12.7mm diameter Aluminum spheres were used in addition to solid spheres; the hollow nature of these impactors decreases their relative density by a factor of ~ 4 . The velocity of the ejecta is measured using two noninvasive imaging techniques: 3-dimensional particle imaging velocimetry (3D-PIV) and particle tracking velocimetry (PTV) of the ejecta curtain profile. The 3D-PIV technique allows characterization of the non-axisymmetric ejecta flow field that results from oblique impacts, while the PTV enables the determination of very high ejection velocities over a wider range of ejection angles. The 3D-PIV and PTV data sets were recorded at high speeds (10,000 and $\sim 11,000$ frames per second, respectively), thereby allowing for time-resolved examination of ejecta flow field.

Analysis and Results: The scaled velocity distributions of the hollow and solid projectiles are closely

matched at early stages of the cratering process; the downrange results (representing the ejecta with the highest speed) are presented here (see Fig.1). The upturn of the slope of the velocity at early stages indicates a departure from main-stage power-law excavation flow. This initial high-speed component, composed of mostly fine material, is characterized by a fairly small amount of mass relative to the total ejected volume. The ejection angles of this early-time component sweep upward about 10° to the nominal ejection angle of $\sim 45^\circ$ for sand (see Fig.2) for the solid projectile. The hollow projectile exhibits lower ejection angles, consistent with a shallower coupling depth[5]. Lunar stimulant (JSC-1a) displays even lower ejection angles under the same conditions.

These non-dimensional results can be scaled to the size of the LCROSS event to find the ejecta curtain radius at various heights above the impact (Fig.3). Since the impact will occur in a shadowed area, the ejecta will not be visible until it attains a sufficient height to be illuminated by the sun (i.e. above a crater rim). The curtain radius is thus considered as a function of time after impact (TAI), where $TAI = t_{launch} + t_{ballistic}$, the sum of the time between impact and ejecta launch and the ballistic time of flight. The delay in arrival time of the ejecta at various heights can be measured in the tens of seconds.

Conclusions: Based on comparisons with sand, the initial stage of the EDUS impact will generate a low mass, low angle, high velocity component at early stages. Similar impacts into JSC-1a yield even lower ejection angles than the sand target. These results affect extrapolations based on standard ejecta scaling during the early stages of growth. These experiments into sand are a first step in understanding the ejecta velocity distribution of the LCROSS mission. Extension to other materials, such as JSC-1a, is essential for a more complete picture of the impact event. Coupling the velocity with the time-resolved mass ejected will yield the mass-velocity distribution.

References:

- [1] Korycansky, D.G., Plesko, C.S., *et al.* (2008) in *LPSC* vol. 39 1963. [2] Shuvalov, V.V., Trubetskaya, I.A. (2008) *Solar System Research* 42, 1–7. [3] Heldmann, J.L., Colaprete, T., *et al.* (2007) in *LPSC* vol. 38 1369.
- [4] Schultz, P.H. (2006) *LPI Contributions* 1327, 14–15.
- [5] Anderson, J.L.B., Schultz, P.H., *et al.* (2003) *JGR(Planets)* 108, 5094. [6] Housen, K.R., Schmidt, R.M., *et al.* (1983) *JGR* 88, 2485–2499.

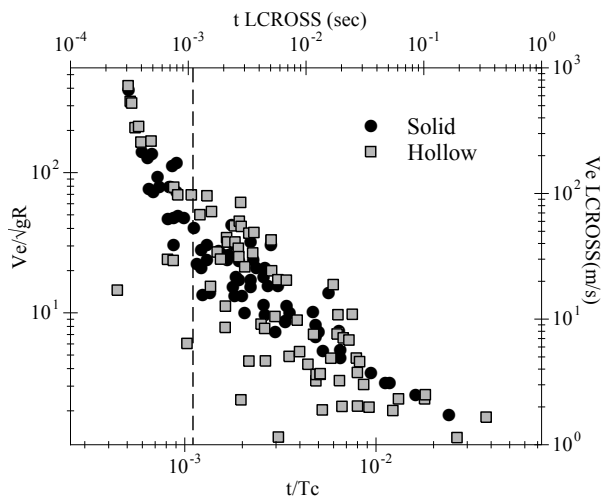


Figure 1: Dimensionless velocity vs. time. Downrange component. Both the hollow and solid Al spheres display an augmented ejection speed very early on in the cratering process before evolving into main-stage power-law growth as predicted by dimensional analysis[6]. Ejection velocity (right axis) and time(top axis) have been scaled to the LCROSS event for comparison. Dashed line approximates time of $V_e=300\text{m/s}$.

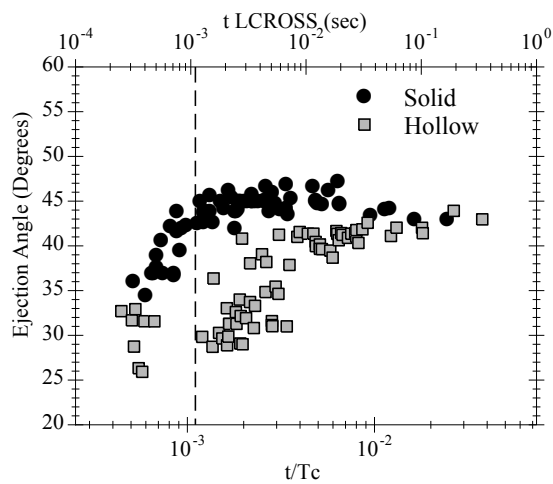


Figure 2: Ejection Angles. Data presented is downrange component of ejecta curtain. Ejection angles start out low, then sweep upward to the $\sim 45^\circ$ angle predicted for impacts in sand[6]. Ejection angles from hollow sphere are more chaotic in the early stages due to the failure of the projectile, and are characteristically lower than the solid sphere. These measurements were taken of the leading edge (and thus the lowest ejection angle) of the curtain using the PTV technique. Dashed line approximates time of $V_e=300\text{m/s}$.

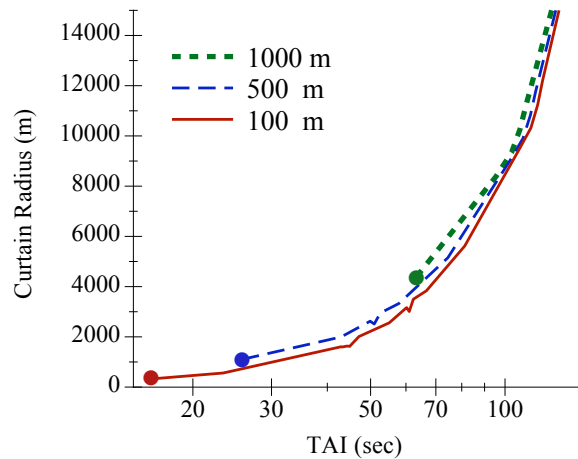


Figure 3: LCROSS Predicted Curtain Radius. Semilog plot. The ejecta curtain radius is scaled to the LCROSS event assuming a crater radius of 17m, calculated for different heights above the impact surface. Dots correspond to first light for ballistic ejecta rising above the shadow line for each curve. The delay between impact and first arrival of ejecta at each height is $\propto \sqrt{\text{height}}$.

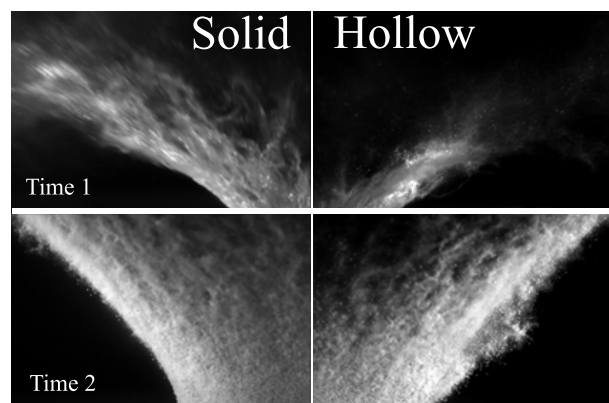


Figure 4: Comparison of ejecta profiles with varying projectile density. Two sets of images (at ~ 0.350 and ~ 32 msec after impact) of the downrange portion of the ejecta curtain profile (perpendicular to impact vector) for the solid (left) and hollow (right) projectiles at 2.0 km/s at 60° into #20-30 sand. Images of the impact of the hollow projectile are reflected along the vertical axis to emphasize symmetry.